Alasemenia, the earliest ovule with three wings and without cupule

Deming Wang[1,6,*], Jiangnan Yang[1,6], Le Liu[2,6], Yi Zhou[3], Peng Xu[1], Min Qin[4,*], Pu Huang[5]

[1]Key Laboratory of Orogenic Belts and Crustal Evolution, Department of Geology, Peking University, Beijing 100871, China.

[2]School of Geoscience and Surveying Engineering, China University of Mining and Technology (Beijing), Beijing 100083, China.

[3]School of Life Sciences, Sun Yat-Sen University, Guangzhou 510275, China.

[4]College of Life Sciences, Linyi University, Linyi 276000, China.

[5]Nanjing Institute of Geology and Palaeontology, Chinese Academy of Sciences, Nanjing 210008, China.

[6]these authors contributed equally.

*email: dmwang@pku.edu.cn, qinmin1990@yeah.net

The ovules or seeds (fertilized ovules) with wings are widespread and especially important for wind dispersal. However, the earliest ovules in the Famennian of the Late Devonian are rarely known about the dispersal syndrome and usually surrounded by a cupule. From Xinhang, Anhui, China, we report a new taxon of Famennian ovules, *Alasemenia tria* gen. et sp. nov. Each ovule possesses three integumentary wings evidently extending outwards, folding inwards along abaxial side and enclosing most part of nucellus. The ovule is borne terminally on smooth dichotomous branches and lacks a cupule. *Alasemenia* suggests that the integuments of the earliest ovules without a cupule evolved functions in wind dispersal and probable photosynthetic nutrition. It indicates that the seed wing originated earlier than other wind dispersal mechanisms such as seed plume and pappus, and that three- or four-winged seeds were followed by seeds with less wings. Mathematical analysis shows that three-winged seeds are more adapted to wind dispersal than seeds with one, two or four wings under the same condition.

Introduction

Since plants colonized the land, wind dispersal (anemochory) became common with the seed wing representing a key dispersal strategy through geological history (Taylor et al., 2009; Ma, 2009; Stephen and Christian, 2019). Winged seeds evolved numerous times in many lineages of extinct and extant seed plants (spermatophytes) (Schenk, 2013; Stevenson et al., 2015). Lacking wings as integumentary outgrowths, the earliest ovules in the Famennian (372-359 million years ago [Ma], Late Devonian) rarely played a role in wind dispersal (Rowe, 1997). Furthermore, nearly all Famennian ovules are cupulate, i.e., borne in a protecting and pollinating cupule (Prestianni et al., 2013; Meyer-Berthaud et al., 2018).

Warsteinia was a Famennian ovule with four integumentary wings, but its attachment and cupule remain unknown (Rowe, 1997). *Guazia* was a Famennian ovule with four wings and it is terminally borne and acupulate (devoid of cupule) (Wang et al., 2022). This paper documents a new Famennian seed plant with ovule, *Alasemenia tria* gen. et sp. nov. It occurs in Jianchuan mine of China, where Xinhang fossil forest

was discovered to comprise in situ lycopsid trees of *Guangdedendron* (Wang et al., 2019). The terminally borne ovules are three-winged and clearly acupulate, thus implying additional or novel functions of integument. Based on current fossil evidence and mathematical analysis, we discuss the evolution of winged seeds and compare the wind dispersal of seeds with different number of wings.

Results

Locality and stratigraphy

All fossils came from Upper Devonian Wutong Formation at Jianchuan mine in Xinhang town, Guangde City, Anhui Province, China. Details on locality are available in previous works (Wang et al., 2019; Xu et al., 2022). At this fossil locality, Wutong Formation consists of Guanshan Member with quartzose sandstone and a little mudstone, and the overlying Leigutai Member with inter-beds of quartzose sandstone, siltstone and mudstone. Spore analysis indicates that the Leigutai Member here is late Famennian in age (Gao et al., 2023). Progymnosperm *Archaeopteris* and lycopsid *Leptophloeum* occur in Leigutai and/or Guanshan members, and they were distributed worldwide in the Late Devonian (Taylor et al., 2009). Fernlike plant *Xinhangia* (Yang and Wang, 2022) and lycopsid *Sublepidodendron* (Xu et al., 2022) were found at the basal part of Leigutai Member. In situ lycopsid trees of *Guangdedendron* with stigmarian rooting system appear in multiple horizons of Leigutai Member and they formed the Xinhang forest (Wang et al., 2019; Gao et al., 2022). From many horizons of siltstone and mudstone of Wutong Formation (Leigutai Member) at Jianchuan mine, numerous ovules of *Alasemenia* were collected.

Systematic palaeontology

Division Spermatophyta

Order and family incertae sedis

Alasemenia tria gen. et sp. nov.

Etymology

The generic name from the Latin “ala” and “semen”, meaning wing and seed, respectively; the specific epithet from the Latin “tri” (three), referring to wing number of a seed.

Holotype designated here

PKUB21721a, b (part and counterpart housed in Department of Geology, Peking University, Beijing) (Fig. 1a, m, n).

Locality and horizon

Xinhang, Guangde, Anhui, China; Leigutai Member of Wutong Formation, Upper Devonian.

Diagnosis

Dichotomous branches bearing terminal and acupulate ovules. Three broad wing-like integumentary lobes radially and symmetrically attached to each nucellus, distally tapered and proximally reduced. Integumentary lobes evidently extending outwards, with their free parts ca. 40% of ovule length. Individual integumentary lobes folding inwards along abaxial side. Nucellus largely adnate to integument.

Description

Some ovules are borne terminally on smooth branches that are thrice (Fig. 1a), twice (Fig. 1c) or once (Fig. 1b, f, g, i; Fig. 2a-c) dichotomous at 40-135°. The boundary between ovule and ultimate axis below refers to position where the ovule width just begins to increase (e.g., Fig. 1a, arrow). The branches excluding ovules are up to 76 mm long and 0.4-0.9 mm wide. Most ovules terminate ultimate axis (Fig. 1j, 2d-f) or are detached (Fig. 1d, e, h, k, 2g-o). The ovules are 25.0-33.0 mm long and 3.5-5.6 mm at the maximum width (excluding the width of outward extension of integumentary wings). Compressions of ovules (Fig. 1-3) and their serial transverse sections (Fig. 4; Fig. S1-5) do not show any cupules.

Each ovule possesses a layer of integument with three radially arranged and wing-like integumentary lobes (Fig. 1a, d, e, 2d, e, o, arrows, 3a-f, 4; Fig. S1-5). They are broad, acropetally tapered and proximally reduced to merge with the ultimate axis (Fig. 1a-c, f, 2a, d-i, n). The integumentary lobes are 1.2-2.3 mm at the maximum width and free for 8.3-14.8 mm distance (32%-45% of the ovule length), and the free lobe parts extend well above the nucellar tip and greatly curve outward. Usually, two lobes of a single ovule are evident and the third one is sometimes exposed through dégagement (Fig. 1a, 2n, arrow 2, o, middle arrow, 3a, e, arrow). Such situation indicates that the lobes of an ovule are present on different bedding planes.

In transverse sections of an ovule, two integumentary lobes extend along the bedding plane, and the third lobe is either originally perpendicular to or compressed to lie somewhat along the bedding plane (Fig. 4c-e, h-k, n-r, t, w-y; Fig. S1-5). The integumentary lobes are narrow, flattened and fused in the lower part of an ovule, and acropetally become wide, thick, separated and far away (Fig. 4c-e; Fig. S1a-k, 2). Because of great outward curving of lobes, it is difficult to observe their distal parts in the sections. When thick, the lobes present a V or U shape. Therefore, they are symmetrically folded along the abaxial side and toward the ovule center.

A few ovules show the outline of a nucellus, which is ca. 10-11.7 mm long and 1.2-1.7 mm at the maximum width (Fig. 1d, 2i, arrows, j, 3f-h). Transverse sections occasionally meet the nucellar tip (Fig. 4d, arrow). With the exception of tip, the nucellus is adnate to the integument and is distally surrounded by the free parts of integumentary lobes.

Discussion

Comparison of winged ovules and record of acupulate ovules in Devonian

In Devonian ovules, besides *Alasemenia*, both *Guazia* (Wang et al., 2022) and *Warsteinia* (Rowe, 1997) possess winged integumentary lobes. As in *Alasemenia*, the lobes of *Guazia* are broad, thin and fold inwards along the abaxial side, but their numbers are four in each ovule and their free portions usually arch centripetally. In contrast to *Alasemenia*, *Warsteinia* has four integumentary lobes and their free portions are short, flat and straight.

Except few taxa including *Guazia* (Wang et al., 2022), *Dorinnotheca* (Fairon-Demaret, 1996), *Cosmosperma* (Liu et al., 2017), *Elkinsia* (Serbet and Rothwell, 1992) and *Moresnetia* (Fairon-Demaret and Scheckler, 1987), the earliest ovules in the

Famennian (Late Devonian) do not have branches connected. Now, as in *Guazia*, the ovules of *Alasemenia* terminate the dichotomous branches and are transversely sectioned to show the ovular structures. The ovules of these two genera provide evidence for acupulate ovules in the earliest seed plants.

Functions of Devonian acupulate ovules and evolution of winged ovules

Both cupule and integument of an early ovule perform the protective and pollinating functions (Meyer-Berthaud, 2022). The integument of *Alasemenia* is adnate to most part of the nucellus and its three lobes extend long distance above the nucellar tip and then evidently outwards. Such structure leads to efficient protection of nucellus and adaptation for pollination. Little is known about the dispersal syndrome of Famennian ovules, because the wings as a derived character are rarely documented. *Guazia*, *Warsteinia*, and now *Alasemenia* indicate that the anemochory originated in Famennian. Their integumentary wings illustrate diversity in number (three or four per ovule), length, folding or flattening, and being straight or curving distally. *Alasemenia* confirms that, like *Guazia*, the integuments of acupulate ovules developed a new function in wind dispersal.

In early seed plants, the fertile branches terminated by ovulate cupules consistently lack leaves and thus the cupules probably serve a nutritive function as in photosynthetic organs; this function may be transferred to the integuments of acupulate ovules such as *Guazia* (Meyer-Berthaud, 2022). Of *Alasemenia*, the nutritive function would also apply to the integuments since the acupulate ovules are terminal on various orders of naked branches and ultimate axes. The surface of integuments is enlarged through the outgrowths of wings and thus promotes the photosynthesis.

Alasemenia, *Guazia* and *Warsteinia* suggest that the evolutionarily novel wings, as integument outgrowths and the most important mechanism for seed dispersal by wind, appeared early in the spermatophytes and had been manifested in younger lineages. Other wind dispersal mechanisms including plumes, pappi and parachutes of seeds appeared later in the Permo-Carboniferous and Mesozoic, respectively (Axsmith et al., 2013). Current evidence indicates that seeds with three or four wings occurred first in the Late Devonian. They were followed by two- or three-winged seeds in the Carboniferous (Long, 1960, 1969), and then by single-winged seeds in the Permian (Stevenson et al., 2015; Prevec et al., 2008). Relating to wind dispersal, the diaspores (seeds/fruits) of living spermatophytes possess multiple mechanisms and variable number of wings (Ma, 2009).

Ovules of *Alasemenia* and *Guazia* terminating long and narrow branches suggest easy abscission of diaspores (ovules with or without an ultimate axis) and better preparation for dispersal. Compared to *Warsteinia* with short and straight wings and *Guazia* with long but inwards curving wings, *Alasemenia* with long and outwards extending wings would efficiently reduce the rate of descent and be more capably moved by wind.

Mathematical analysis of wind dispersal of ovules with 1-4 wings

The rate of diaspore descent in still air is an important indicator of the potential ability of modern samaras dispersal (Augspurger et al., 2016, 2017). In examining samaras, it has been demonstrated that the value of angular velocity is smaller than that

of terminal velocity (Green, 1980), and the relationship between the samaras' wing loading and terminal velocity v_{ter} is:

$$v_{\mathrm{ter}} \propto \sqrt{\frac{w}{A_w}}$$

where w is the weight of samaras, A_W is the surface area of the wing, w/A_W is defined as the samaras' wing loading.

As for ovules, we also use terminal velocity as an indicator of dispersal ability. Since the broad integumentary wings well extend outwards, the wing loading of *Alasemenia* is obviously less than that of *Guazia*. When the winged seeds fall in the air, the predictable spinning can lead to the reduction of fall rate, and result in the increase of the horizontal dispersal distance. This has been observed in the field experiments or proved in the modelling reconstruction experiments (Green, 1980; Habgood et al., 1998).

However, the tiny asymmetry of ovules will be amplified in the running geometry by centrifugal and aerodynamic loads, result in vibrations and thus significantly reduce the efficiency (Lu et al., 2019). The transverse wave caused by vibrations will arrive the tip of wing and form stationary waves. In the ovules with even number of wings like *Guazia* (Wang et al., 2022) and *Warsteinia* (Rowe, 1992, 1997), the center symmetry structure will lead to stronger resonance than the ovules with odd number of wings (like *Alasemenia*). It means the ovules with odd number of wings are more stable in high rate spinning and spend more falling time in the dispersal process.

Another consideration is the capacity of airflow in horizontal direction. The Reynolds number (Re) is the indicator of patterns in fluid flow situations, and for ovules, the Reynolds numbers are mainly fall in 10^3-10^4, suggesting that the inertia forces are much stronger than viscous forces (Burrows, 1975; Seter and Rosen, 1992). In this situation, the thrust of airflow can be represented as:

$$F = c\rho v^2 S$$

where c is the coefficient, ρ is the density of air, S is the windward face, v is the velocity of relative movement.

It means that we can transform the comparison of capacity of airflow into the area of windward. Supposing the maximum windward area of each wing is S_{wing} and n represents the number of wings revolving on its own axis, we define a function $S(\theta)$ to represent the area of windward when the angle between airflow and wings is θ. We introduce relative efficiency E_r for comparison. Here we list 5 ideal basic situations. The summary results are shown in Fig. 5.

1. $n = 2$ and the wings keep facing the wind (wings without rotation, as a control group). In this situation, the area of windward is identical to $2S_{wing}$, which can be written as:

$$S(\theta) = 2S_{wing},\ \theta \in [0, 2\pi]$$

$$(\text{If } n = 1,\ S(\theta) = S_{wing},\ \theta \in [0, 2\pi])$$

We define a function $D(\theta)$ to represent the accumulated area of windward in a cycle. By definition,

$$D(\theta) = 2\pi\, S(\theta) = 4\pi S_{wing},$$

$$E_r = 100\%$$

2. $n = 2$. In this situation, we discuss the condition when $\theta \in [0,\ \pi]$.

$$S(\theta) = 2\sin\theta\, S_{wing} \in \left[0, 2S_{wing}\right]$$

Based on symmetry,

$$D(\theta) = 2\int_0^{\pi} S(\theta)d\theta = 4S_{wing}\int_0^{\pi} sin\,\theta\, d\theta = 4S_{wing}(\cos 0 - \cos\pi) = 8S_{wing},$$

$$E_r = 8S_{wing}/4\pi S_{wing} \approx 63.66\%$$

3. $n = 1$. In this situation,

$$S(\theta) = \sin\theta\, S_{wing} \in \left[0, S_{wing}\right],$$

$$D(\theta) = 4S_{wing},$$

As can be seen in Fig. 5, the relative efficiency is equal to the situation of $n = 2$,

$$E_r \approx 63.66\%$$

4. $n = 3$ (*Alasemenia*).

$$S(\theta) = 2(\sin\theta + \sin\left(\frac{2\pi}{3} - \theta\right) S_{wing} = 2S_{wing}\, sin\frac{\pi}{6} cos\left(\frac{\pi}{3} - \theta\right),$$

$$S(\theta) = \sqrt{3}S_{wing}\, cos\left(\frac{\pi}{3} - \theta\right) \in \left[\frac{3S_{wing}}{2}, \sqrt{3}S_{wing}\right],\ \theta \in [\pi/6, \pi/3].$$

Based on symmetry,

$$D(\theta) = 12\int_{\frac{\pi}{6}}^{\frac{\pi}{3}} S(\theta)d\theta = 12\sqrt{3}S_{wing}\left(\sin\frac{\pi}{6} - \sin 0\right) = 6\sqrt{3}S_{wing},$$

$$E_r = 6\sqrt{3}S_{wing}/4\pi S_{wing} \approx 82.70\%$$

5. $n = 4$ (*Guazia*, *Warsteinia*).

$$S(\theta) = 2S_{wing}\max(\sin\theta, \cos\theta),\ \theta \in [0, \pi/2]$$

When $\theta \in [\pi/4, \pi/2]$,

$$S(\theta) = 2S_{wing}\sin\theta \in \left[\sqrt{2}S_{wing}, 2S_{wing}\right]$$

Based on symmetry,

$$D(\theta) = 8 \times 2S_{wing}\int_{\frac{\pi}{4}}^{\frac{\pi}{2}} sin\,\theta\, d\theta = 16S_{wing}\left(\cos\frac{\pi}{4} - \cos\pi\frac{\pi}{2}\right) = 8\sqrt{2}S_{wing},$$

$$E_r = 8\sqrt{2}S_{wing}/4\pi S_{wing} \approx 90.03\%.$$

Generally, the above one- to four- winged seeds are quantitatively analysed for their wind dispersal capability and the results are shown in Fig. 5. The relative efficiency (E_r) of these seeds in five ideal basic situations are calculated for comparison.

The one- or two- winged seeds are treated as a control group when the wings keep facing the wind and do not rotate. In this case, the relative efficiency for wind dispersal is 100%. In descending through autorotation, one- to four-winged seeds present different relative efficiencies for wind dispersal.

In summary, the mathematical analysis of winged seeds indicates that the relative wind dispersal efficiency of three-winged seeds is obviously better than that of single- and two- winged seeds, and is close to that of four-winged seeds (Fig. 5). In addition, the maximum windward area of each wing of *Alasemenia* is greater than that of *Guazia* and *Warsteinia* with four wings. Significantly, three-winged seeds have the most stable area of windward, which also ensures the motion stability in wind dispersal. All these factors suggest that *Alasemenia* is well adapted for anemochory.

References

Augspurger, C. K., Franson, S. E., Cushman, K. C., & Muller-Landau, H. C. (2016). Intraspecific variation in seed dispersal of a Neotropical tree and its relationship to fruit and tree traits. *Ecology and Evolution* **6**, 1128-1142.

Augspurger, C. K., Franson, S. E., & Cushman, K. C. (2017). Wind dispersal is predicted by tree, not diaspore, traits in comparisons of Neotropical species. *Functional Ecology* **31**, 808-820.

Axsmith, B. J., Fraser, N. C. and Corso, T. A. (2013). Triassic seed with an angiosperm-like wind dispersal mechanism. *Palaeontology* **56**, 1173–1177.

Burrows, F. M. (1975). Wind-borne seed and fruit movement. *New phytologist* **75**: 405-418.

Fairon-Demaret, M. (1996). *Dorinnotheca streelii* Fairon-Demaret, gen. et sp. nov., a new early seed plant from the upper Famennian of Belgium. *Rev. Palaeobot. Palynol.* **93**, 217-233.

Fairon-Demaret, M., and Scheckler S.E. (1987). Typification and redescription of *Moresnetia zalesskyi* Stockmans, 1948, an early seed plant from the Upper Famennian of Belgium. Bull. Inst. R. Sci. Nat. Belg. 57, 183-199.

Gao, X. et al. (2022). Re-study of *Guangdedendron micrum* from the Late Devonian Xinhang forest. *BMC Evol. Biol.* **22**, 69.

Gao, X., Ji, X.-K., Zhou, Y., Yang, J.-N., and Wang, D.-M. (2023). Spore assemblage from the Upper Devonian Wutong Formation in Xinhang, Anhui. *Acta Scientiarum Naturalium Universitatis Pekinensis* 59, 221-230.

Green, D.S. (1980). The terminal velocity and dispersal of spinning samaras. *American Journal of Botany* **67**: 218-1224.

Habgood, K. S., Hemsley, A. R., & Thomas, B. A. (1998). Modelling of the dispersal of *Lepidocarpon* based on experiments using reconstructions. *Review of Palaeobotany & Palynology* **102**: 101-114.

Liu, L., Wang, D.-M, Meng, M-C., and Xue, J-Z. (2017). Further study of Late Devonian seed plant *Cosmosperma polyloba*: Its reconstruction and evolutionary significance. *BMC Evol. Biol.* **17**, 149.

Long, A. G. (1960). On the structure of *Samaropsis scotica* Calder (emended) and *Eurystoma angulare* gen. et sp. nov., petrified seeds from the calciferous sandstone of Berwickshire. *Trans. Roy. Soc. Edin.* **64**, 261–280.

Long, A. G. (1969). VII.—*Eurystoma trigona* sp. nov., a pteridosperm ovule borne on a frond of *Alcicornopteris* Kidston. *Trans. Roy. Soc. Edin.* **68**, 171–182.

Lu, Y., Lad, B., Vahdati, M., & Stapelfeldt, S. C. Nonsynchronous vibration associated with transonic fan blade untwist. In Turbo Expo: Power for Land, Sea, and Air. 2019; Vol. 58684, p. V07AT36A013. American Society of Mechanical Engineers.

Ma W.-L. (2009). *Botany* (Higher Education Press, Beijing).

Meyer-Berthaud, B., Gerrienne, P., and Prestianni, C. (2018). Letters to the twenty-first century botanist. Second series: "what is a seed?" – 3. How did we get there? Palaeobotany sheds light on the emergence of seed. *Bot. Lett.* **165**, 434-439.

Prestianni, C, Hilton, J, and Cressler, W. (2013). Were all Devonian seeds cupulate? A reinvestigation of *Pseudosporogonites hallei*, *Xenotheca bertrandii*, and *Aglosperma* spp. Int J Plant Sci 174, 832-851.

Prevec, R., McLoughlin, S., and Bamford, M. K. (2008). Novel double wing morphology revealed in a South African ovuliferous glossopterid fructification: *Bifariala intermittens* (Plumstead 1958) comb. nov. *Rev. Palaeobot. Palynol.* **150**, 22–36.

Rowe, N. P. (1992). Winged Late Devonian seeds. *Nature* **359**, 682.

Rowe, N. P. (1997). Late Devonian winged preovules and their implications for the adaptive radiation of early seed plants. *Palaeontology* **40**, 575-595.

Schenk, J. J. (2013). Evolution of limited seed dispersal ability on Gypsum islands. *Am. J. Bot.* **100**, 1811–1822.

Serbet, R., and Rothwell, G. W. (1992). Characterizing the most primitive seed ferns. I. A reconstruction of *Elkinsia polymorpha*. *Int. J. Plant Sci.* **153**, 602-621.

Seter, D. & Rosen, A. (1992). Study of the vertical autorotation of a single winged samara. *Biological Reviews* **67**: 175-197.

Stephen, M., Christian, P. (2019). Plant mobility in the Mesozoic: Disseminule dispersal strategies of Chinese and Australian Middle Jurassic to Early Cretaceous plants. *Palaeogeogr. Palaeoclimatol. Palaeoecol.* **515**, 47–69.

Stevenson, R. A., Evangelista, D. and Looy, C. V. (2015). When conifers took flight: a biomechanical evaluation of an imperfect evolutionary takeoff. *Paleobiology* **41**, 205-225.

Taylor, T. N., Taylor, E. L., and Krings, M. (2009). *Paleobotany: The Biology and Evolution of Fossil Plants* (2nd ed, Academic Press, Burlington).

Wang, D-M. et al. (2019). The most extensive Devonian fossil forest with small lycopsid trees bearing the earliest stigmarian roots. *Curr. Biol.* **29**, 2604-2615.

Wang, D.-M. et al. (2022). *Guazia*, the earliest ovule without cupule but with unique integumentary lobes. *Natl. Sci. Rev.* **9**, nwab196.

Xu, P., Liu, L., and Wang, D.-M. (2022). Reinvestigation of the Late Devonian lycopsid *Sublepidodendron grabaui* from Anhui Province, South China. *Biology* **11**, 1544.

Yang, J.-N., and Wang, D.-M. (2022). A new fern-like plant *Xinhangia spina* gen. et sp. nov. from the Upper Devonian of China. *Biology* **11**, 1568.

Methods

All specimens are housed in Department of Geology, Peking University, Beijing, China. Steel needles were used to expose some seeds and fertile axes. Serial dégagement was employed to reveal the morphology and structure of seeds. Seeds were embedded in resin, sectioned and ground to show the integuments and nucelli. All

photographs were made with a digital camera and microscope.

Acknowledgements

We thank X. Gao, Z. Z. Deng and L. Liu for help in fieldwork. Q. Y. Jia and D. B. Ni provide assistance in the experiment for seed sections. This work was supported by the National Natural Science Foundation of China (grant no. 42130201).

Author Contributions

D.W., L.L. and M.Q. conceived the research. All authors collected the fossils. D.W. and J.Y. conducted the observations and photography of specimens. Y.Z., P.X. and P.H. made mathematical analysis and prepared some figures. D.W. wrote the manuscript, with discussion and contributions from other authors.

Competing interests

The authors declare no competing interests.

Fig. 1. Fertile branches and seeds of *Alasemenia tria* gen. et sp. nov. a, Thrice dichotomous branch with a terminal ovule. Arrow indicating boundary between ovule and ultimate axis (PKUB21721a). **b, f, g, i,** Once dichotomous branch with a terminal ovule (PKUB21781, PKUB23132, PKUB19338a, PKUB17899). **c**, Twice dichotomous branch with a terminal ovule (PKUB19713a). **d, e**, Ovule with three integumentary wings (PKUB19321, PKUB19316). **h,** Ovule showing two integumentary wings (PKUB19282). **j, k,** Ovule terminating short ultimate axis (PKUB23114, PKUB23129). Scale bars, 1 cm (**a-c, h**), 5 mm (**d-g, i-k**).

Fig. 2. Fertile branches and seeds of *Alasemenia tria* gen. et sp. nov. a-c, Once dichotomous branch with a terminal ovule. a, b, Part and counterpart (PKUB16876a, b, PKUB17767). **d, e,** Part and counterpart, arrow showing the third integumentary wing (PKUB19322a, b). **f,** Ovule on ultimate axis (PKUB21752). **g, h, k-m,** Ovules lacking ultimate axis (PKUB16788, PKUB21631, PKUB16522 PKUB21647, PKUB21656). **i, j,** Part and counterpart, showing limit (arrows) between nucellus and integument (PKUB19339a, b). **n,** Four detached ovules (arrows 1-4) (PKUB19331). **o,** Enlarged ovule in n (arrow 2), showing three integumentary wings (arrows). Scale bars, 1 cm (**n**), 5 mm (**a-h, k-m, o**), 2 mm (**i, j**).

Fig. 3. Seeds of *Alasemenia tria* gen. et sp. nov. a, b, Part and counterpart, enlarged ovule in Fig. 1a (PKUB21721a, b). **c,** Enlarged ovule in Fig. 1c. **d,** Counterpart of ovule in c (PKUB19713b). **e,** Dégagement of ovule in d, exposing the base of the third integumentary wing (arrow). **f,** Enlarged ovule in Fig. 1d. **g, h,** Enlarged ovule in Fig. 2i, j, respectively. Scale bars, 5 mm (**a-e**), 2 mm (**f-h**).

Fig. 4. Transverse sections of seeds of *Alasemenia tria* gen. et sp. nov. a, b, Part and counterpart. **c-e,** Sections of seed in a and b (at three lines, in ascending orders). Arrow in d indicating probable nucellar tip (Slide PKUBC17913-12b, 10a, 9b). **f, g,** Part and counterpart. **h-k,** Sections of seed in f and g (at four lines, in ascending orders) (Slide PKUBC19798-8b, 6b, 4a, 4b). **l, m,** Part and counterpart. **n-r,** Sections of seed in l and m (at five lines, in ascending orders), showing three wings departing centrifugally (Slide PKUBC17835-5a, 7b, 8b, 9a, 10a). **s, v, A,** One seed sectioned. **t, u,** Sections of seed in s (at two lines, in ascending orders) (Slide PKUBC18716-8b, 7a). **w-z,** Sections of seed in v (at four lines, in ascending orders) (Slide PKUBC20774-7a, 6b, 3a, 3b). **B-E,** Sections of seed in A (at four lines, in ascending orders), showing three wings departing centrifugally (Slide PKUB17904-5b, 4a, 4b, 3b). Scale bars, 2 mm (**a, b, f, g, l, m, s, v, A**), 1 mm (**c-e, h-k, n-r, t, u, w-z, B-E**).

Fig. 5. The mathematical analysis of wind dispersal ability of ovules with 1-4 wings. The maximum windward area of each wing is S_{wing} and n represents the number of wings per ovule. r is the distance from the tip of wing to the axis of ovules. $S(\theta)$ represents the area of windward when the angle between airflow and wings is θ, and $D(\theta)$ represents the accumulated area of windward in a cycle. $E_r(\%)$ means relative efficiency for wind dispersal. Red lines and expressions show the situation of $n = 1$.

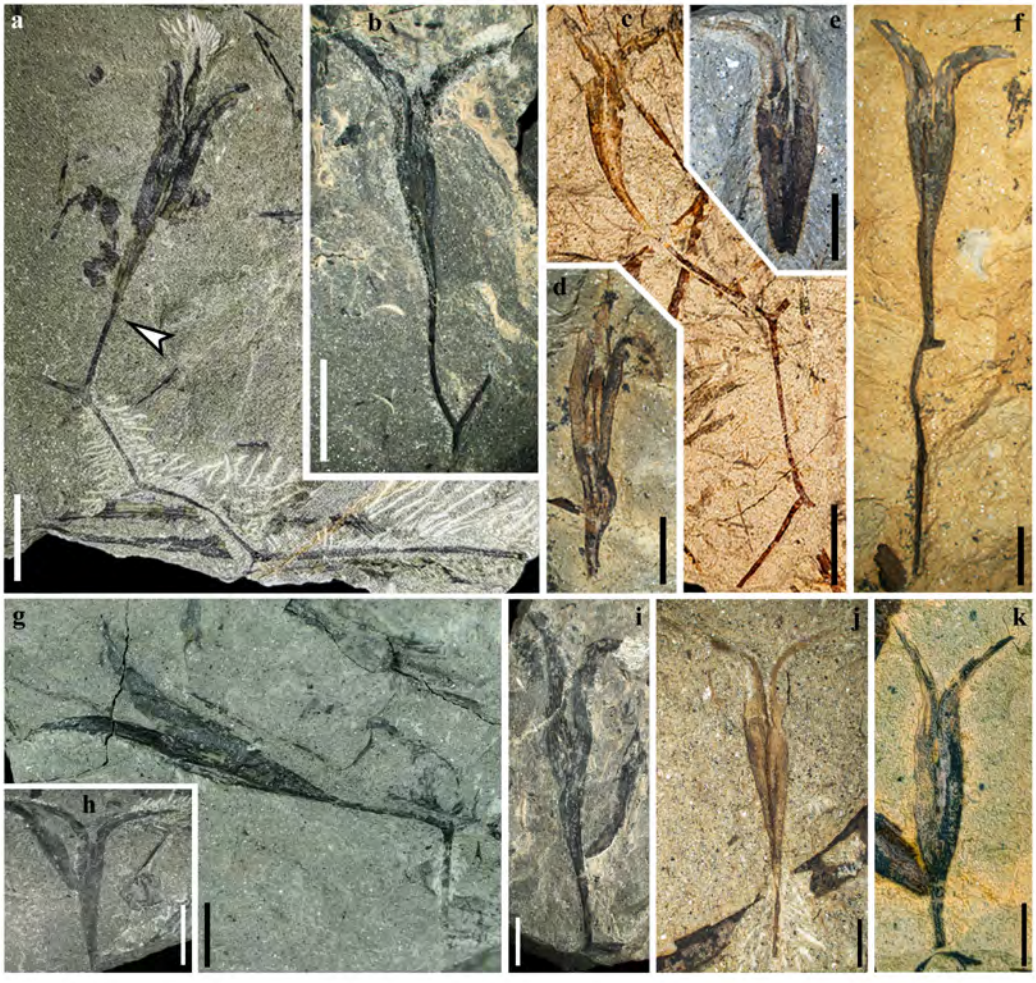

Fig. 1

Fig. 2

Fig. 3

Fig. 4

The number of wings (n)	Top view	Area of windward			Relative efficiency $E_r(\%)$
		S(θ)		$D(\theta)/S_{wing}$	
		Function	Graph		
$n = 2$ $n = 1$ the wings keep facing the wind	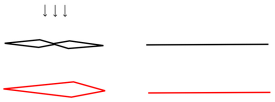	$S(\theta) = 2S_{wing}$, $S(\theta) = S_{wing}$ $\theta \in [0, 2\pi]$.	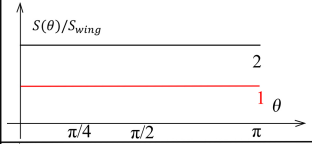	4π 2π	100.0
$n = 2$ $n = 1$	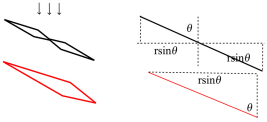	$S(\theta) = 2\sin\theta\, S_{wing}$ $S(\theta) = \sin\theta\, S_{wing}$ $\theta \in [0,\ \pi]$	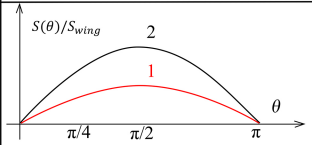	8 4	63.66
$n = 3$ (*Alasemenia*)	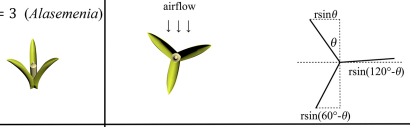	$S(\theta) = \sqrt{3}S_{wing}\cos\left(\frac{\pi}{3} - \theta\right)$ $\theta \in [\frac{\pi}{6}, \frac{\pi}{3}]$	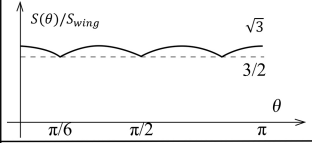	6	82.70
$n = 4$ (*Guazia*)	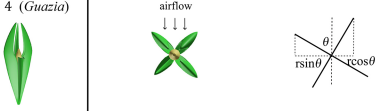	$S(\theta) = 2S_{wing}\max(\sin\theta, \cos\theta)$ $\theta \in [0, \pi/2]$	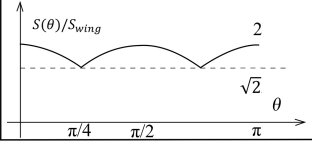	$8\sqrt{2}$	90.03

Fig 5

supplementary information

Alasemenia, the earliest ovule with three wings and without cupule

Deming Wang[1,6,*], Jiangnan Yang[1,6], Le Liu[2,6], Yi Zhou[3], Peng Xu[1], Min Qin[4,*], Pu Huang[5]

[1]Key Laboratory of Orogenic Belts and Crustal Evolution, Department of Geology, Peking University, Beijing 100871, China.

[2]School of Geoscience and Surveying Engineering, China University of Mining and Technology (Beijing), Beijing 100083, China.

[3]School of Life Sciences, Sun Yat-sen University, Guangzhou 510275, China.

[4]College of Life Sciences, Linyi University, Linyi 276000, China.

[5]Nanjing Institute of Geology and Palaeontology, Chinese Academy of Sciences, Nanjing 210008, China.

[6]these authors contributed equally.

*email: dmwang@pku.edu.cn, qinmin1990@yeah.net

Fig. S1. Transverse sections of two seeds of *Alasemenia tria* gen. et sp. nov. a-k, Serial sections of seed in Fig. 3a, b, at eleven levels and in ascending order (Slide PKUBC17913-13b, 12a, 12b, 11a, 11b, 10a, 10b, 9a, 9b, 8a, 8b). **j, k,** Arrows indicating integumentary lobes. **l-x,** Serial sections of seed in Fig. 3f, g, at thirteen levels and in ascending order (Slide PKUBC19798-11a, 9a, 9b, 8a, 8b, 7a, 7b, 6a, 6b, 5a, 5b, 4a, 4b). **c, f, i, p, t, w, x,** The same as those in Fig. 3c-e, h-k, respectively. Scale bars, 1 mm.

Fig. S2. Transverse sections of one seed of *Alasemenia tria* gen. et sp. nov. a-q, Serial sections of seed in Fig. 3l, m, at seventeen levels and in ascending order (Slide PKUBC17835-4b, 4a, 5b, 5a, 6b, 6a, 7b, 7a, 8b, 8a, 9b, 9a, 10b, 10a, 11b, 12a, 12b). **d, g, i, l, n,** The same as those in Fig. 3n-r, respectively. **m-q,** Arrows indicating integumentary lobes. Scale bars, 1 mm.

Fig. S3. Transverse sections of two seeds of *Alasemenia tria* gen. et sp. nov. a-d, Sections of seed in Fig. 3s, at four levels and in ascending order (Slide PKUBC18716-10a, 8a, 8b, 7a). **e-i,** Sections of another seed (at five levels, in ascending order) (Slide PKUBC18984-9b, 8b, 8a, 7b, 7a). **c, d,** The same as those in Fig. 3t, u, respectively. Scale bars, 1 mm.

Fig. S4. Transverse sections of one seed of *Alasemenia tria* gen. et sp. nov. a-l, Serial sections of seed in Fig. 3v, at twelve levels and in ascending order (Slide PKUBC20774-9a, 9b, 8a, 8b, 7a, 7b, 6a, 6b, 5a, 5b, 3a, 3b). **e, h, k, l,** The same as those in Fig. 3w-z, respectively. Scale bars, 1 mm.

Fig. S5. Transverse sections of one seed of *Alasemenia tria* gen. et sp. nov. a-j, Serial

sections of seed in Fig. 3A, at ten levels and in ascending order (Slide PKUBC17904-6a, 6b, 5a, 5b, 4a, 4b, 3a, 3b, 2a, 2b). **d-f, h,** The same as those in Fig. 3B-E, respectively. Scale bars, 1 mm.

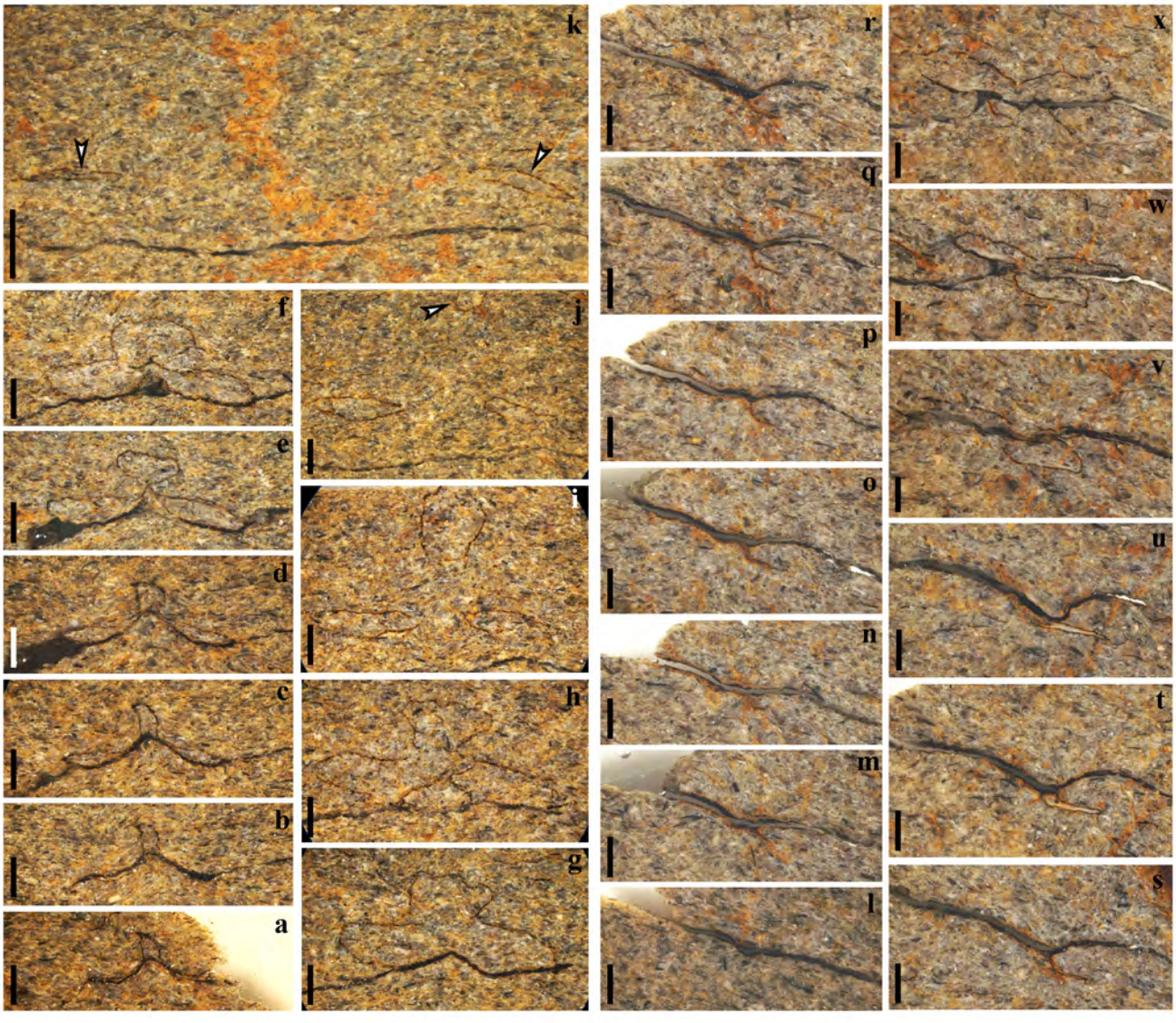

Fig. S1

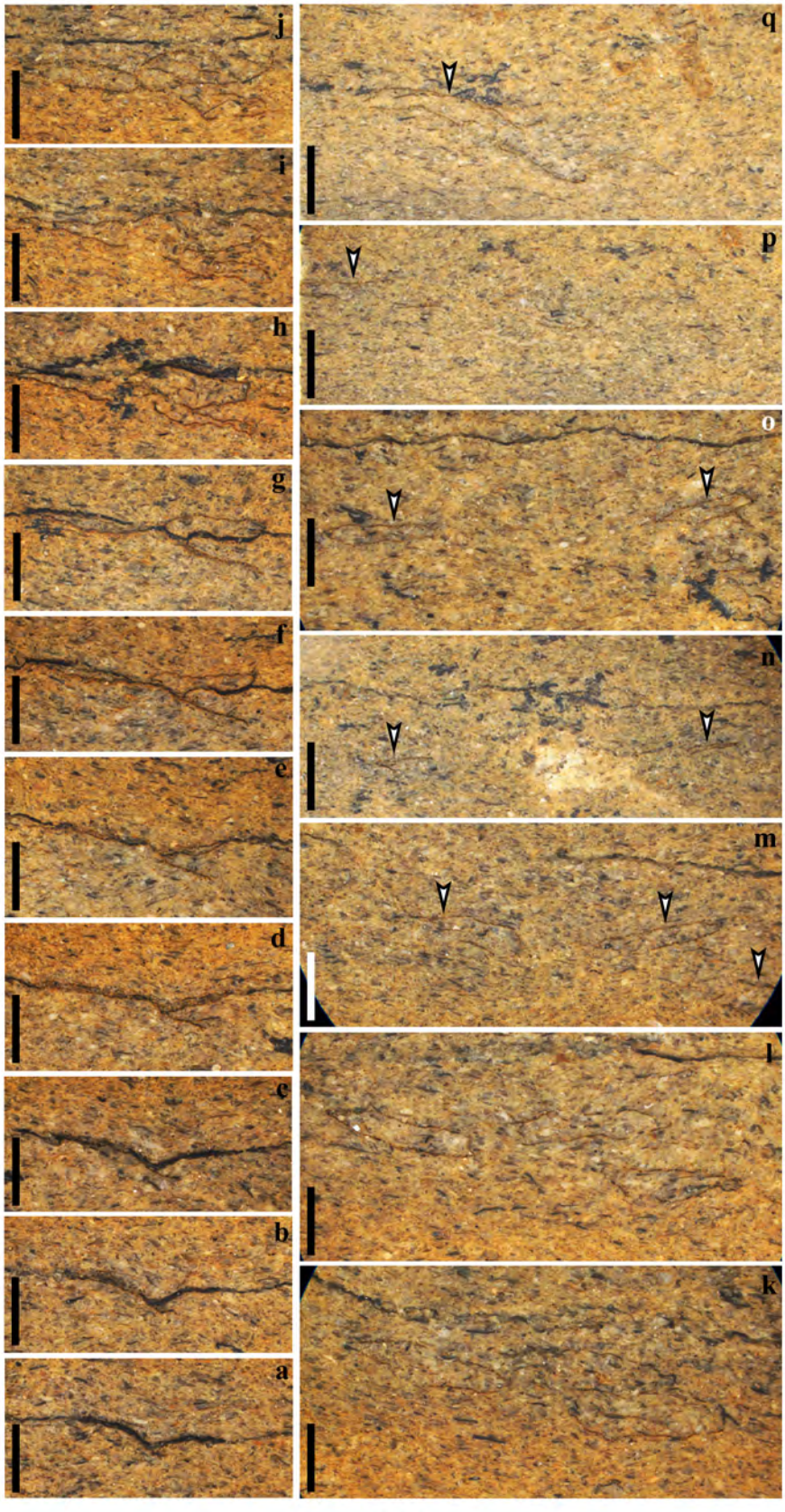

Fig. S2

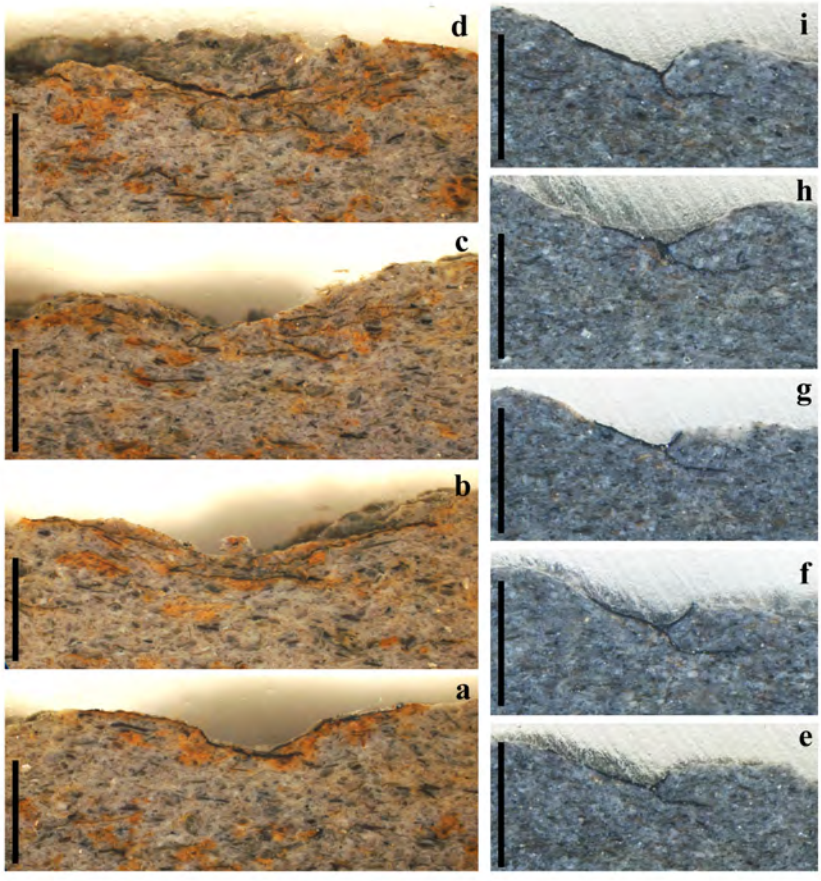

Fig. S3

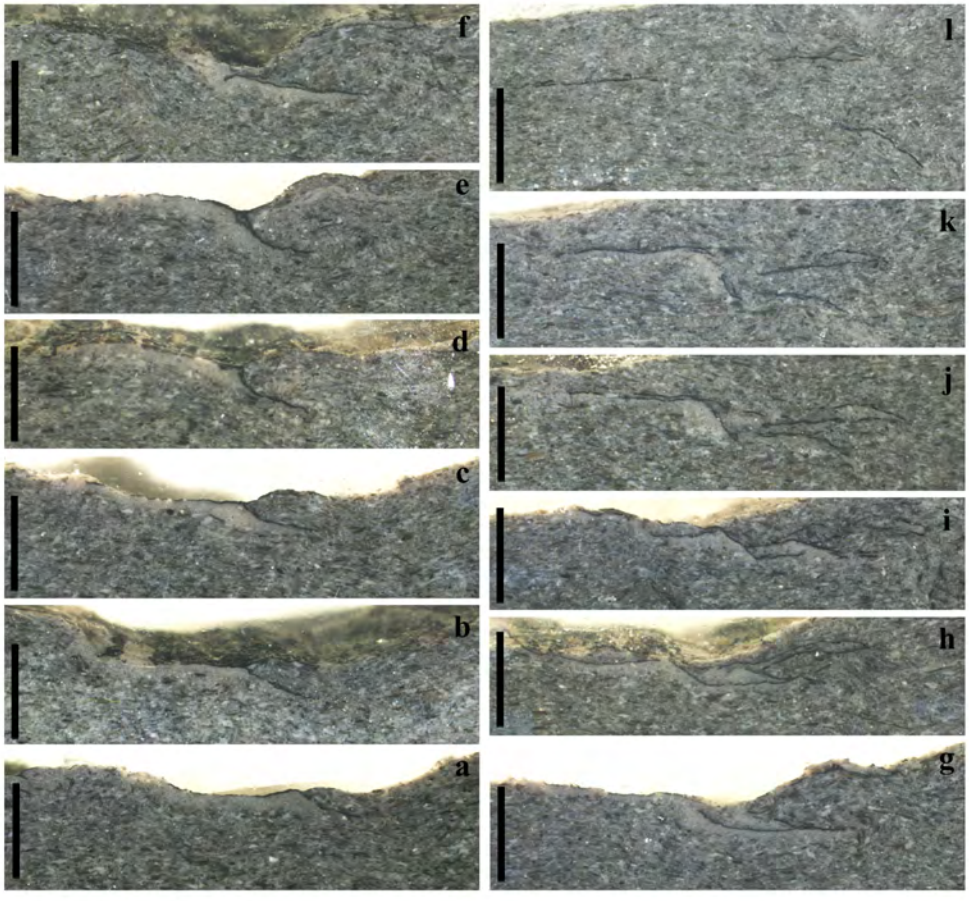

Fig. S4

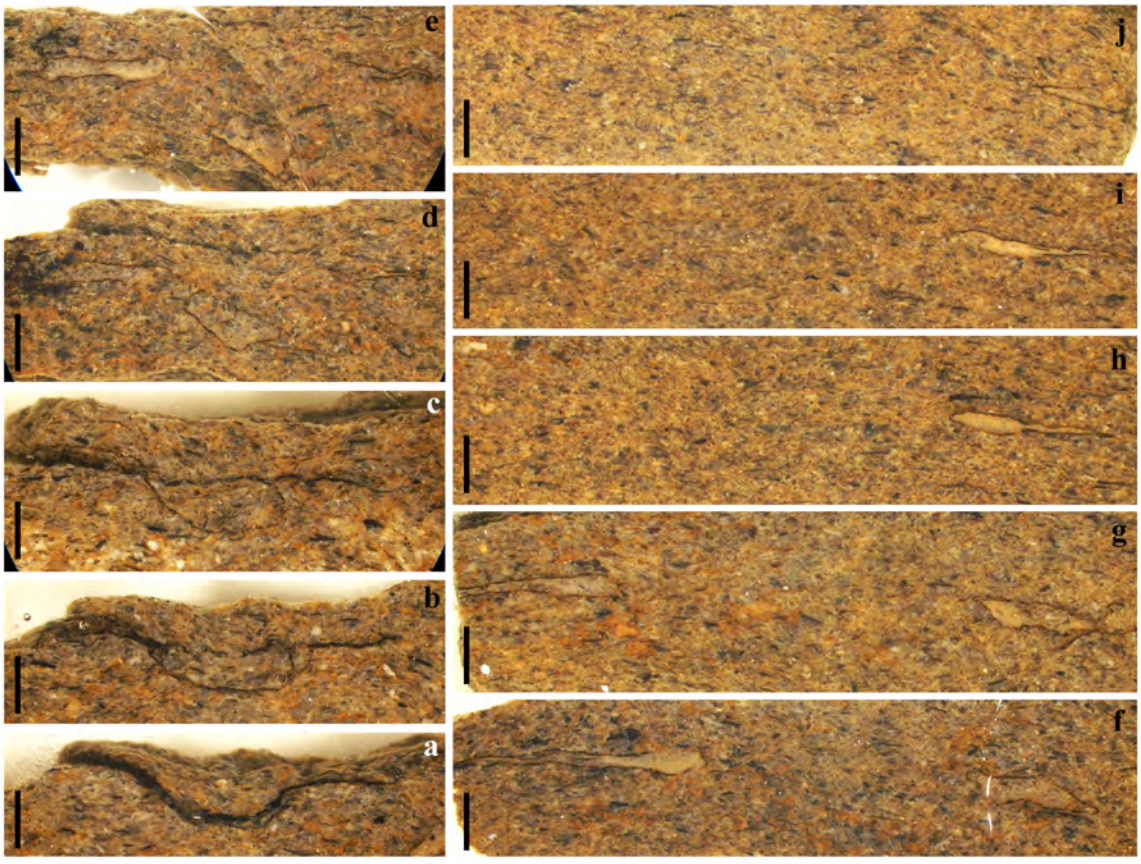

Fig. S5